*354–360* *Nucleic Acids Research, 1996, Vol. 24, No. 2* 

# An oligodeoxyribonucleotide N3′→P5′ phosphoramidate duplex forms an A-type helix in solution

**Daoyuan Ding, Sergei M. Gryaznov[1], David H. Lloyd[1], S. Chandrasekaran, Shijie Yao, Lynda Ratmeyer, Yinquan Pan and W. David Wilson***

Department of Chemistry, Georgia State University, Atlanta, GA 30303, USA and [1]Lynx Therapeutics Inc., 3832 Bay Center Place, Hayward, CA 94545, USA

Received August 21, 1995; Revised and Accepted October 31, 1995

## ABSTRACT

**The solution conformations of the dinucleotide d(TT) and the modified duplex d(CGCGAATTCGCG)$_2$ with N3′→P5′ phosphoramidate internucleoside linkages have been studied using circular dichroism (CD) and NMR spectroscopy. The CD spectra indicate that the duplex conformation is similar to that of isosequential phosphodiester RNA, an A-type helix, and is different from that of DNA, a B-type helix. NMR studies of model dimers d(TpT) and N3′→P5′ phosphoramidate d(TnpT) show that the sugar ring conformation changes from predominantly C2′-endo to C3′-endo when the 3′-phosphoester is replaced by a phosphoramidate group. Two-dimensional NMR (NOESY, DQF-COSY and TOCSY spectra) studies of the duplex provide additional details about the A-type duplex conformation of the oligonucleotide phosphoramidate and confirm that all furanose rings of 3′-aminonucleotides adopt predominantly N-type sugar puckering.**

## INTRODUCTION

Antisense and antigene therapeutic strategies are attractive because they potentially offer highly specific targeting of the nucleic acids of interest (1,2). Such selectivity in action can significantly reduce the toxic side effects observed with other nucleic acid-addressed therapeutic agents. Antisense and antigene compounds developed to this time use Watson–Crick and Hoogsteen nucleobase recognition rules for specificity of interaction with targets and contain nucleosides connected through various linkers (1,2). These linking groups are generally based on structural similarity to the original phosphodiester. Phosphodiester-linked oligonucleotides are too easily degraded by cellular nucleases to be used as *in vivo* therapeutic agents. To date phosphorothioate backbone-modified oligonucleotides have been shown to be one of the best antisense agents and several oligonucleotide phosphorothioates are in clinical trials against a variety of targets (1,3). Typically, however, duplexes and, especially, triplexes formed by phosphorothioate strands are less stable than those derived from corresponding phosphodiesters (4,5). Consequently, it should be possible to improve efficiency in antisense therapeutics by development of modifications that retain the favorable properties of phosphorothioates, such as increased resistance to nuclease degradation, but that have enhanced duplex and triplex stability.

In antisense applications of oligonucleotides their targets are single-stranded RNA regions with the nucleoside C3′-endo sugar conformation and preferences for A-type duplexes. This duplex structure preference could be important in the development of improved antisense agents. There is also evidence that the base stacking in triple helical DNA is closer to an A-type conformation than is observed in DNA duplexes, although many of the sugars retain the C2′-endo conformation (6). These data suggest that oligonucleotides which prefer an A-type conformation in the single-stranded state should provide pronounced enhancements in stability of duplexes with RNA and of triple helixes with duplex DNA.

It was recently reported that oligonucleotides with an internucleoside N3′→P5′ phosphoramidate linkage (Fig. 1) form very stable duplexes and triplexes with complementary nucleic phosphodiester compounds (7,8). The N3′→P5′ phosphoramidate monoester internucleoside linkage is not chiral, is nuclease resistant and has the same formal charge as phosphodiesters. Initial studies with the dinucleoside monophosphate d(TnpA) suggested that the sugar with a 3′-phosphoramidate linkage has a greater percentage of the N conformation (C3′-endo) than sugars with a phosphodiester linkage (7). We have initiated a combined circular dichroism (CD) and NMR study on the duplex d(CGCGAATTCGCG)$_2$ formed by uniformly modified oligonucleotide N3′→P5′ phosphoramidate strands to determine whether the sugar preference for the N conformation will remain in a double-stranded complex and to determine whether the duplex conformation corresponds to an A-helical family. The oligonucleotide sequence d(CGCGAATTCGCG)$_2$ was chosen because its structure has been investigated in detail as DNA and RNA phosphodiesters by X-ray crystallography and NMR methods (9,10). We find that the 3′-amino-substituted nucleosides in the duplex have sugar rings with a high percentage of the N-type conformation and that the duplex adopts an A-type conformation,

* To whom correspondence should be addressed

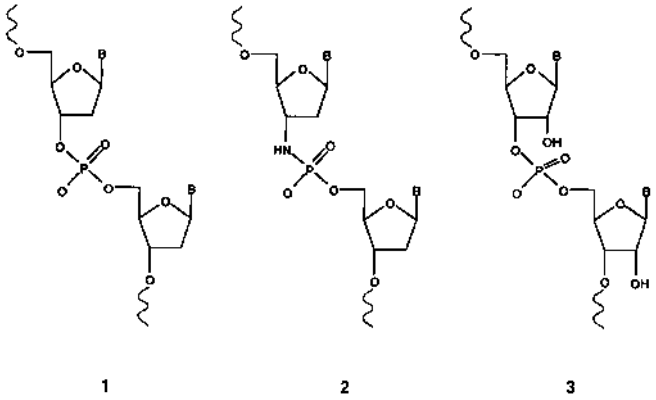

**Figure 1.** Structures of N3′→P5′ phosphoramidate (**2**) and DNA (**1**) or RNA (**3**) phosphodiester linkages.

even though it consists of 2′-deoxyribonucleosides. To our knowledge this is the first report of a mixed sequence duplex formed by 2′-deoxynucleosides with a phosphate-based backbone that adopts the A conformation in solution under physiologically relevant conditions.

## MATERIALS AND METHODS

### Materials

Thymidine ($dT_{OH}$) and the dimer d(TpT) were purchased from Sigma (St Louis, MO). The phosphoramidate and phosphodiester oligonucleotides used in this research were synthesized, purified and characterized as previously described (7,8).

### Thermal denaturation experiments

Thermal denaturation experiments were conducted on a Cary 4 spectrophotometer, as previously described (11), in 0.01 M PIPES buffer, pH 7.0, containing 1 mM EDTA, 0.1 M NaCl and $6 \times 10^{-6}$ M nucleic acid strand concentration. $T_m$ values were determined by fitting the data with a non-linear least squares computer program that includes sloping base lines in the duplex and single-strand regions.

### CD spectra

CD spectra were obtained with a JASCO J-710 spectrophotometer interfaced to an IBM computer as previously described (12). CD experiments were conducted at temperatures from 15 to 90°C in 1 cm path length cuvettes with a buffer adjusted to pH 7.0 containing 3.75 mM $NaH_2PO_4$, 1 mM EDTA, 0.1 M NaCl and $2.1 \times 10^{-6}$ M strand concentration. Phosphate buffer was substituted for PIPES buffer in order to obtain CD spectra at lower wavelengths.

### NMR spectroscopy

The samples were dissolved in 0.6 ml 99.96% $D_2O$ or 90% $H_2O$ solution containing 7.5 mM phosphate, 0.01 mM EDTA, 100 mM NaCl, pH 7.0. All NMR spectra were acquired with a Varian Unity plus 600 MHz spectrometer at 25°C, except for the temperature study of the phosphoramidate duplex, which was obtained with a Varian Unity plus 500 MHz spectrometer. The one-dimensional (1D) NMR data were processed by Vnmr 4.3 software from Varian. The two-dimensional (2D) NMR data were transferred to a Silicon Graphics work station and processed with Felix 2.3 software from Biosym. 1D spectra were collected with a spectral width of 5000 Hz and 32K data points. A 2D NOESY spectrum at 300 ms mixing time was acquired using 90% $H_2O$ as solvent with spectral widths of 14 000 Hz in D1 and 7198 Hz in D2 and data sizes of 4096 points in *t*2 and 512 in *t*1. Data were zero-filled to 4K points in both dimensions. A 2D NOESY spectrum at 100 ms mixing time was recorded with a spectral width of 5000 Hz in both dimensions and 4096 data points in *t*2, 512 in *t*1. After zero-filling a data set of 4K × 4K was obtained. The double-quantum filtered COSY (DQF-COSY) spectrum was collected with a spectral width of 5000 Hz in both dimensions and 4096 data points in *t*2, 512 in *t*1. The *t*2 dimension was then zero-filled to 4K. The TOCSY spectrum was obtained using a spin-lock time of 40 ms with 5000 Hz spectral width in both dimensions and 2048 data points in *t*2, 512 in *t*1, zero-filled to 2K × 2K. All 2D NMR data were acquired in the phase-sensitive mode using the States–Haberkorn method of phase cycling and were apodized with a sine-bell function shifted by 90°.

## RESULTS

### Duplex stability

Melting curves for the sequence CGCGAATTCGCG as oligonucleotide RNA, DNA and N3′→P5′ phosphoramidate are shown in Figure 2A and illustrate the remarkable stability of the phosphoramidate duplex. The melting studies were repeated at several salt concentrations and the $T_m$ values are plotted as a function of log[$Na^+$] in Figure 2B. The lines have similar slopes of 16 ± 2. It is clear from these results that substitution of the N3′→P5′ phosphoramidate linkages for phosphodiesters significantly stabilizes the nucleic acid duplex at all salt concentrations used and the effect of increasing salt concentration for the phosphoramidate duplex is very similar to that for DNA and RNA. The $T_m$ curve for the phosphoramidate duplex is steeper than for the phosphodiester duplexes and this suggests that a greater enthalpy component is, at least partially, responsible for the increased stabilization of the modified duplex.

### Sugar ring conformation in dinucleosides

NMR studies have been conducted with the phosphoramidate-substituted dinucleoside monophosphate d(TnpT), where np indicates the N3′→P5′ phosphoramidate linkage, with the d(TpT) phosphodiester as a reference. The percentage of N conformer was evaluated from the standard two-state N–S deoxyribose equilibrium assumption using the Karplus equation as modified by Altona and co-workers (13). In d(TnpT) the nucleoside linking group is the N3′→P5′ phosphoramidate, while the 3′-terminal nucleoside has a 3′-OH group. Significant differences in vicinal hydrogen coupling constants between the two 2′-deoxyriboses in the phosphoramidate dimer are apparent in the H1′ spectral region of the NMR spectrum (Fig. 3). In the 3′-amino nucleoside no significant coupling between H1′ and H2′ protons was observed, indicating that the dihedral angle between H1′ and H2′ is close to 90°, as expected for the C3′-endo conformation (10,13). In contrast, significant coupling for the same protons was observed in the 3′-terminal nucleoside (Table 1), indicating a significantly higher percentage of the C2′-endo conformation. The increase in

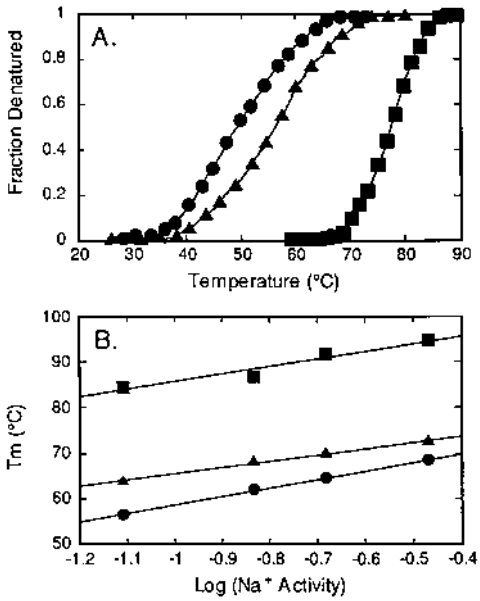


**Figure 2.** (**A**) Thermal melting curves for phosphodiester DNA (●) and RNA (▲) and phosphoramidate DNA (■). Measurements were determined in PIPES buffer, 0.1 M NaCl and $6.0 \times 10^{-6}$ M strand concentration. (**B**) $T_m$ versus log[$Na^+$] for phosphodiester DNA (●), RNA (▲) and phosphoramidate DNA (■). Measurements were obtained in PIPES buffer, $6 \times 10^{-6}$ M strand concentration and varying amounts of NaCl.

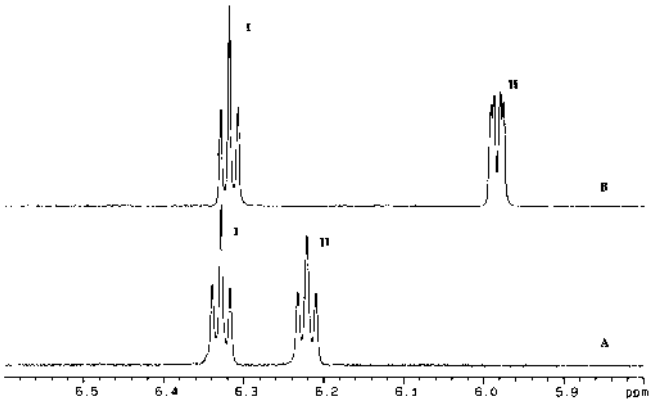


**Figure 3.** The 600 MHz proton spectra (H1′ region) of dimers (**A**) d(TpT) and (**B**) d(TnpT). The peaks I and II were assigned to 3′-terminal (dpT, dnpT) and 5′-terminal (dTp, dTnp) residues respectively, according to their 2D COSY spectra.

percentage of the N conformation in the dinucleoside for the 3′-amino- versus 3′-hydroxyl-substituted sugar correlates with the trend observed for 3′-$NH_2$ versus 3′-OH mononucleosides, where replacement of a 3′-hydroxyl by an amino group increases the amount of C3′-endo conformation (Table 1) (14). These results indicate that in the dimer the nucleoside sugar puckers are relatively independent and the sugar conformation is strongly affected by changes in the 3′ substituent (14).

**Table 1.** The sums of H1′ coupling constants (Hz), Σ1′ and populations of N-type conformer for thymidine ($T_{OH}$), 3′-aminothymidine ($T_{NH2}$), dTpT, dTnpT and phosphoramidate duplex $d(CGCGAATTCGCG)_2$[a]

| | | Σ1′[b] | Fraction N conformation[c] |
|---|---|---|---|
| $T_{OH}$ | | 13.6 | 0.4 |
| $T_{NH2}$ | D2O | 12.0 | 0.8 |
| | Buffer[a] | 12.3 | 0.8 |
| | DMSO | 12.0 | 0.8 |
| d(TpT) | dTp | 13.8 | 0.3 |
| | dpT | 13.4 | 0.4 |
| d(TnpT) | dTnp | 9.4 | ~1.0 |
| | dnpT | 13.8 | 0.3 |
| Duplex | C1 | 7.3 | ~1.0 |
| | G2 | 6.8 | ~1.0 |
| | C3 | 7.2 | ~1.0 |
| | G4 | 7.4 | ~1.0 |
| | A5 | 6.8 | ~1.0 |
| | A6 | 8.5 | ~1.0 |
| | T7 | 9.3 | ~1.0 |
| | T8 | 8.9 | ~1.0 |
| | C9 | 7.4 | ~1.0 |
| | G10 | 6.9 | ~1.0 |
| | C11 | 7.4 | ~1.0 |
| | G12 | 12.2 | 0.6 |

[a]The buffer used was 7.5 mM phosphate, 0.01 mM EDTA, 100 mM NaCl, pH 7.0, except as noted.
[b]Σ1′ = J1′2′ + J1′2″, Σ1′ values of nucleosides and dimers were obtained from the 1D spectra by spin simulation using Vnmr 4.3 software. Σ1′ for the oligomer were obtained from its DQF-COSY spectrum.
[c]Estimated from coupling constants as described (13,14).

## Structure of the N3′→P5′ phosphoramidate duplex

1D NMR spectra of the N3′→P5′ phosphoramidate duplex $d(CGCGAATTCGCG)_2$ as a function of temperature are shown in Figure 4. As can be seen from the melting curve in Figure 2, the phosphoramidate sample is in the duplex state below 70°C and is completely melted above 90°C at $6 \times 10^{-6}$ M strand concentration. The signals in 1D NMR spectra from 25 to 55°C sharpen as expected, due to increased thermal motion in the duplex, and exhibit some small spectral shifts, due to changes in base stacking and end fraying of the duplex, with increasing temperature. At 65°C the signals begin to broaden again, due to intermediate exchange between the duplex and single strands. At 85°C the signals are very broad, due to the exchange process between populations of native and denatured strands (15).

Base and H1′ protons of the N3′→P5′ phosphoramidate duplex $d(CGCGAATTCGCG)_2$ were readily assigned from NOESY spectra by the sequential NOE connectivities in the nucleotide sequence (Fig. 5) (16). Connectivities to the upfield H2′ and H2″ protons from each H1′ served to assign these additional sugar resonances (Table 2). Since the H1′–H2″ distance is fairly constant and is always shorter than the H1′–H2′ distance (16), the H2′ and H2″ protons were distinguished based on the greater

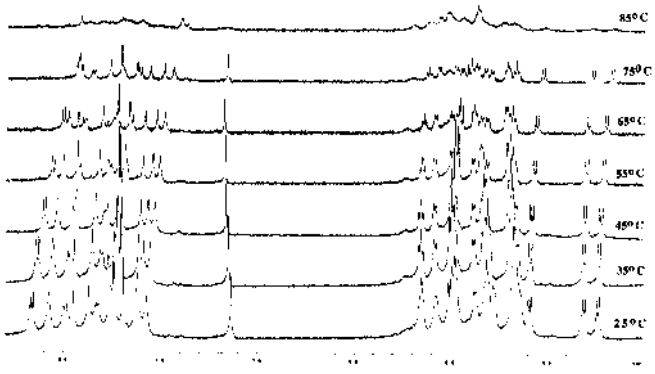

**Figure 4.** The 500 MHz proton spectra of d(CGCGAATTCGCG)$_2$-phosphoramidate (aromatic and H1′ regions) at various temperatures.

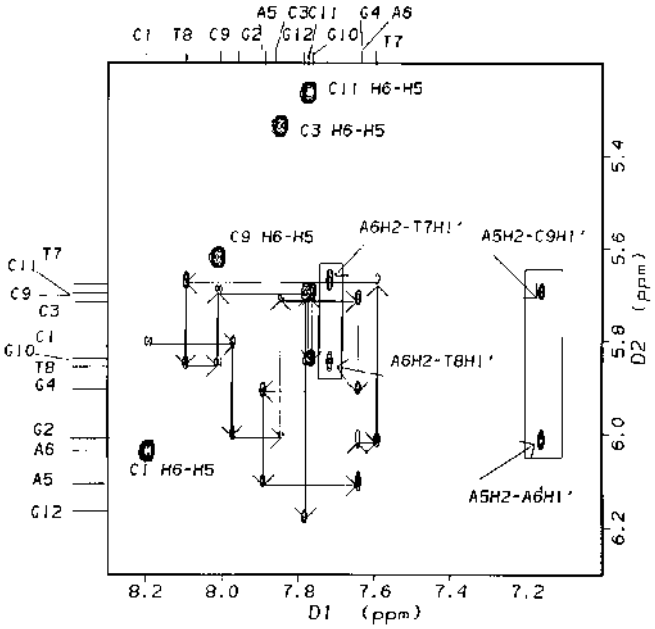


**Figure 5.** Expanded NOESY (600 MHz) spectrum with a mixing time of 300 ms of the aromatic to H1′ region of N3′→P5′ phosphoramidate d(CGCGAATTCGCG)$_2$. The NOE connectivities are traced sequentially from C1 to G12 through each base and sugar. The strong cross-peaks between A5H2 and C9H1′, A5H2 and A6H1′, A6H2 and T7H1′, A6H2 and T8H1′ are shown in the boxed region.

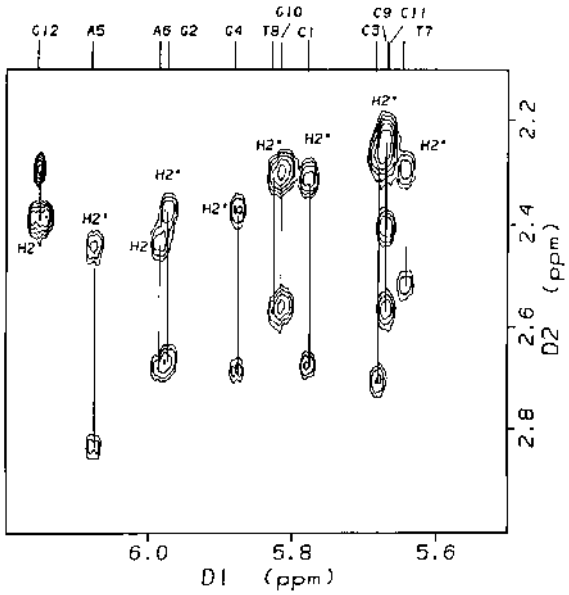


**Figure 6.** An expanded NOESY (600 MHz) spectrum of the H1′ to H2′/H2″ region for the phosphoramidate DNA at a mixing time of 100 ms. In each pair of cross-peaks the more intense ones are from H1′ to H2″, because of the shorter distance between H1′ and H2″, H2′ protons are downfield from H2″, except in the terminal G12, which does not have a phosphoramidate group attached to the 3′ position in the sugar ring.

cross-peak intensity for H1′–H2″ (Fig. 6). Connectivities for H1′–H3′ and H4′ in TOCSY spectra were used to assign the H3′ and H4′ signals (not shown). It is interesting that, unlike DNA phosphodiesters (16), the H3′ proton signals of the phosphoramidate duplex are all upfield of those for H4′, except for G12, which has a 3′-OH and has H3′ downfield of H4′. Other signals, except for several H5′ and H5″ that have not yet been assigned due to extensive overlap, were assigned by NOESY connectivities to the previously identified proton signals (Table 2).

Several additional cross-peaks provided key information for determination of the helical conformational family for the phosphoramidate duplex. Distances from purine H8 or pyrimidine H6 to pyrimidine H5 protons in right-handed helical structures give cross-peaks in NOESY spectra (16) and such a cross-peak is seen from G2H8 to C3H5 in Figure 5. The G10H8–C11H5 cross-peak is too close to the intense C11H5–H6 cross-peak to be observed. Cross-peaks are also seen from A6H8 to the methyl group of T7 and from T7H6 to T8-methyl, as expected for a right-handed helix (not shown). Very important interstrand cross-peaks for specifying the helical family are seen from adenosines AH2 to cross-strand H1′ protons (10): A5H2–C9H1′ and A6H2–T8H1′ (Fig. 5). Intrastrand cross-peaks are observed from A5H2 to A6H1′ and from A6H2 to T7H1′. The H8/H6–H2′/H2″ cross-peaks are also key signals for specifying the helical family. In A-form duplexes the H6/H8 aromatic protons are closer to the H2′/H2″ protons of the preceding sugar ($n$ – 1) than to their own H2′/H2″ protons ($n$) (10,16) and, as demonstrated in Figure 7, in the phosphoramidate duplex the only strong cross-peaks observed are from H8/H6 to the $n$ – 1 H2′/H2″ protons. If the NOESY spectrum is plotted close to the background level weak cross peaks from the H8/H6 protons of the base to the $n$ H2′/H2″ of the sugar protons can be seen, as expected for C3′-endo sugars.

As also expected for N sugar conformations, no H1′–H2′ cross-peaks are observed in DQF-COSY spectra of the phosphoramidate CGCGAATTCGCG duplex for all 3′-amino nucleosides (Fig. 8). In contrast, cross-peaks from H1′ to H2′ and H2” of the terminal G12 are observed (Fig. 8), indicating that the G12 sugar, which has a 3′-OH group, has a higher percentage of the C2′-endo conformation than the other sugar rings of the duplex. It can thus be concluded that the predominant conformation of all nucleoside sugar rings with a 3′-phosphoramidate linkage is C3′-endo, similar to the results described above for the dinucleosides. With the duplex there is no observable H1′–H2′ coupling and the sugar conformation is apparently shifted even more strongly to the C3′-endo range than with the dimer.

**Table 2.** Assignment (in p.p.m.) of proton resonances of phosphoramidate-modified DNA d(CGCGAATTCGCG)$_2$

| | H6/H8 | H1′ | H2′ | H2″ | H3′ | H4′ | H5′/H5″ | H5/CH3 | H2 |
|---|---|---|---|---|---|---|---|---|---|
| C1 | 8.19 | 5.80 | 2.70 | 2.34 | 3.68 | 3.93 | 4.03/4.07 | 6.03 | |
| G2 | 7.98 | 5.99 | 2.70 | 2.40 | 3.86 | 4.04 | 4.13/4.24 | | |
| C3 | 7.85 | 5.71 | 2.74 | 2.30 | 3.69 | 4.00 | 4.10/4.23 | 5.34 | |
| G4 | 7.64 | 5.90 | 2.70 | 2.40 | 3.73 | 4.03 | | | |
| A5 | 7.90 | 6.10 | 2.89 | 2.42 | 3.79 | 4.08 | 4.10/4.25 | | 7.16 |
| A6 | 7.64 | 6.01 | 2.71 | 2.46 | 3.56 | 4.08 | | | 7.72 |
| T7 | 7.59 | 5.67 | 2.55 | 2.32 | 3.62 | 4.02 | 4.06/4.22 | 1.18 | |
| T8 | 8.10 | 5.84 | 2.59 | 2.32 | 3.80 | 4.00 | 4.11/4.23 | 1.56 | |
| C9 | 8.02 | 5.69 | 2.59 | 2.31 | 3.70 | 3.97 | 4.09/4.23 | 5.62 | |
| G10 | 7.77 | 5.84 | 2.58 | 2.30 | 3.73 | 3.98 | 4.07/4.18 | | |
| C11 | 7.78 | 5.70 | 2.58 | 2.43 | 3.70 | 4.00 | | 5.26 | |
| G12 | 7.78 | 6.18 | 2.32 | 2.42 | 4.54 | 4.12 | | | |

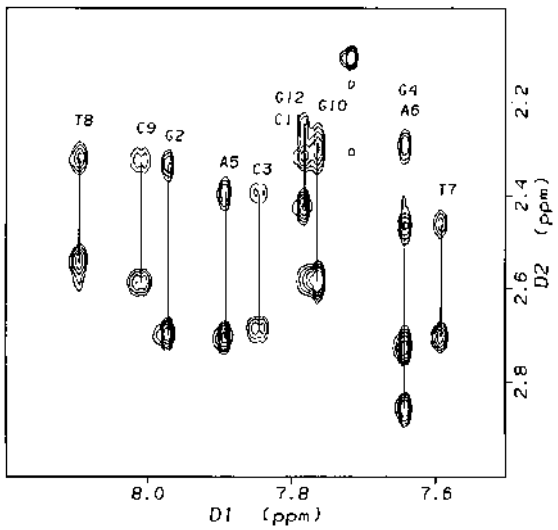


**Figure 7.** An expanded NOESY (600 MHz) of the aromatic to H2′/H2″ region for d(CGCGAATTCGCG)$_2$-phosphoramidate. The vertical lines connect the cross-peaks which correspond to the aromatic protons to *n* – 1 H2′/H2″ NOE. The labels show the chemical shifts of aromatic protons of the bases.

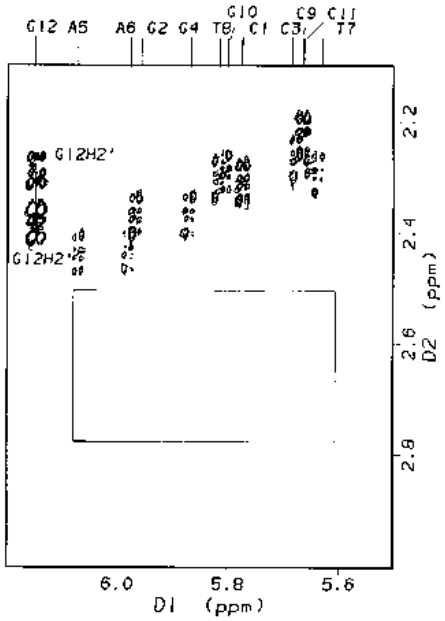


**Figure 8.** Expanded phase-sensitive DQF-COSY (600 MHz) spectrum of the H1′ to H2′/H2″ region for phosphoramidate DNA. The absence of cross-peaks from H1′ to H2′ in the boxed region shows that the sugars adopt predominantly a C3′-endo geometry and the DNA is in an A-form conformation.

## CD spectroscopy

The CD spectra for phosphodiester DNA and RNA duplexes are characteristic of the general B-type and A-type conformations respectively (17–19). In the base absorption region the DNA duplex has a positive CD band near 280 nm, while the RNA duplex has a larger positive band that is shifted to near 260 nm. The spectrum of the N3′→P5′ phosphoramidate is much more similar to that of the RNA spectrum, with a large positive band at 265 nm (Fig. 9). Spectra of both RNA and DNA duplexes have negative bands near 210 nm, but the magnitude of the RNA band is larger than that of the DNA band. Again, in this region the CD spectrum of the phosphoramidate duplex is much more similar to that for RNA than for DNA. Finally, the negative band usually present in B-form CD spectra, at ~250 nm, is absent in RNA CD spectra and is very small in the spectrum of the phosphoramidate duplex. It is clear that the CD results for the phosphoramidate duplex place it in the A-form classification at temperatures below its melting temperature.

To determine how much of the observed CD spectral difference between DNA and the phosphoramidate is intrinsic and how much is due to the base stacking and helical conformation, the duplexes were heated through the $T_m$ region. As can be seen from Figure 9, the spectra for the denatured samples are very similar,

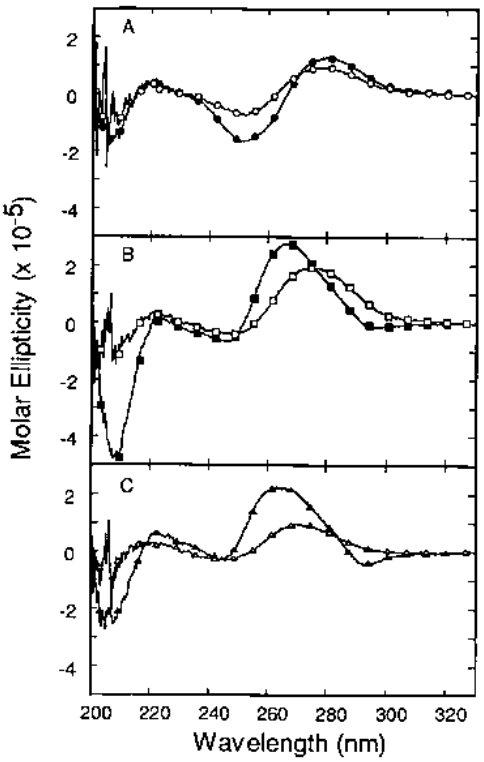


**Figure 9.** CD spectra for native (solid symbols, 25°C) and denatured (open symbols, 95°C) phosphodiester DNA (**A**) and RNA (**C**) and phosphoramidate DNA (**B**). Measurements were conducted in $NaH_2PO_4$ buffer, 0.1 M NaCl and $2.1 \times 10^{-6}$ M strand concentration.

with a positive peak at 275 nm and negative signals at ~250 and 210 nm that have similar intensities in the DNA, RNA and phosphoramidate oligomers.

## DISCUSSION

CD spectra for the oligomer CGCGAATTCGCG as DNA, RNA and N3′→P5′ phosphoramidate are very similar above the $T_m$. At temperatures below the duplex $T_m$ values the CD intensities increase and the spectrum for RNA corresponds to a classic A-type helical pattern, while the spectrum for the DNA duplex shows a B-form helical pattern. The CD spectrum for the phosphoramidate at low temperature is very similar to the RNA A-type pattern and is quite different from the B-helical spectrum (Fig. 9). These experiments indicate that at high temperatures the oligonucleotides are in a similar conformational state as denatured single strands, but both RNA and phosphoramidate assume an A-type of helix in the duplex form while the DNA exists as a B-type duplex below the $T_m$. The results for RNA and DNA are expected (9,10), but the result for the phosphoramidate is somewhat surprising for a 2′-deoxyribose-containing structure. Since the DNA and phosphoramidate duplexes have the same sequence and 2′-deoxyribose sugars, their conformational differences must be caused by substitution of nucleoside 3′-amino for 3′-hydroxy groups.

NMR and X-ray studies on the DNA duplex have demonstrated that it has a B-type conformation, while experiments with the isosequential RNA counterpart have indicated that it has an A-type duplex structure (9,10,20, and references therein). The NMR data presented here for the phosphoramidate duplex strongly support the conclusions from CD experiments that this nucleic acid adopts an A-type helical structure. Analysis of coupling constants indicates that all of the nucleoside 2′-deoxyriboses with a 3′-amino substituent have predominantly N sugar conformations (Table 1). The fact that no H1′–H2′ coupling can be detected (Fig. 8) suggests that all of the 3′-amino sugars are close to a pure N-type conformation. NOESY connectivities also strongly support an A-type conformation. In a duplex with the C3′-endo sugar ring conformation base H6/H8 aromatic protons are close to the $n-1$ sugar H2′/H2″ protons, while in a duplex with nucleoside C2′-endo conformations the aromatic protons are close to the $n$ sugar H2′ and the $n-1$ sugar H2″ protons. The strong H8/H6 cross-peaks observed with the phosphoramidate duplex are all to the $n-1$ H2′/H2″ protons, while much weaker cross-peaks can be seen to the $n$ H2′/H2″, in support of an A-form helical structure (Fig. 7). A particularly important cross-peak for defining the A-form geometry is observed from AH2 to the interstrand $m+1$ residue H1′ (where $m$ refers to the complementary strand). This distance is long in B-form helical conformations (10,16) and no or a weak cross-peak is usually observed. Strong interstrand cross-peaks are observed for A5H2–C9H1′ and A6H2–T8H1′ in the phosphoramidate duplex and confirm that the grooves in the duplex have a characteristic A-form helical topology, as observed in the r(CGCGAAUUCGCG)$_2$ sequence (10). From these NMR and CD spectral data it may be concluded that in the N3′→P5′ phosphoramidate duplex both base stacking and sugar conformation are characteristic of the A-type helical family.

Duplexes with electronegative substituents at the 2′ position, such as RNA, are generally found in an A-form conformation. DNA, with a 2′-deoxysugar can adopt either the A- or B-helical conformation, but in solution the B-form conformation is observed under a wide range of conditions that bracket those observed in biological systems (21). Analysis of substituent effects at the 3′ position of 2′,3′-dideoxyribose derivatives by Chattopadhyaya and co-workers (14, and references therein) has indicated that as a consequence of the gauche effect there is a trend in the sugar conformation from the S conformational state with very electronegative substituents (for example -OH, -F, -$NO_2$) to an N conformational preference as the electronegativity is decreased (for example -H and -$NH_2$ 3′-substituents). We have conducted studies with the dinucleotide monophosphate d(TnpT), which has a N3′→P5′ phosphoramidate linkage and a terminal nucleoside with a 3′-hydroxyl group. The results for the two nucleosides in d(TnpT) are different: the 2′-deoxyribose substituted with a 3′-NH is strongly biased to the N conformational state while that with the 3′-OH has a much higher percentage of the S conformation, as do both nucleosides in the phosphodiester dimer d(TpT) (Table 1). These results indicate that substitution of the normal DNA phosphodiester by the N3′→P5′ phosphoramidate linkage strongly biases the nucleoside sugar puckering to the N state, as expected from the gauche effect. This sugar conformation preference must account for a large part of the observed A-type conformational preference of the phosphoramidate duplex. Our analysis, however, suggests that the percentage N sugar puckering is higher in the phosphoramidate duplex than in the TnpT dimer and it is possible that there are additional structural or functional (e.g. hydration) constraints for the phosphoramidate group in the duplex that act in a cooperative fashion to shift the conformation even more strongly to an A-form helix.

## ACKNOWLEDGEMENTS

This research was supported by NIH grants AI-27196 and AI-33363 and Lynx Therapeutics Inc. The NMR, UV-visible and CD instruments were purchased through funds from the NSF and the Georgia Research Alliance. We appreciate some early spectra in this project that were provided by Dr George Gray of Varian Associates.

## REFERENCES

1 Crooke,S.T. and Lebleu, B. (1993) *Antisense Research and Applications.* CRC Press, Boca Raton, FL.
2 Thuong,N.T. and Hlne,C. (1993) *Angew. Chem. Int. Edn English*, **32**, 666–690.
3 Bayever,E., Iversen,P.L., Bishop,M.R., Sharp,J.G., Teasary,H.K., Arneson,M.A., Pirruccello,S.J., Ruddon,R.W., Kessinger,A., Zon,G and Armitage,J.O. (1993) *Antisense Res. Dev.*, **3**, 383–390.
4 Kibler-Herzog,L., Zon,G., Uznanski,B., Whittier,G. and Wilson,W.D. (1991) *Nucleic Acids Res.*, **19**, 2979–2986.
5 Wilson,W.D., Mizan,S., Tanious,F.A., Yao,S. and Zon,G. (1994) *J. Mol. Recognition*, **7**, 89–98.
6 Radhakrishnan,I. and Patel,D.J. (1994) *Biochemistry*, **33**, 11405–11416
7 Gryaznov,S.M. and Chen,J.-K. (1994) *J. Am. Chem. Soc.*, **116**, 3143–3144.
8 Gryaznov,S.M., Lloyd,D.H., Chen,J.-K., Schultz,R.G., DeDionisio,L.A., Ratmeyer,L. and Wilson,W.D. (1995) *Proc. Natl. Acad. Sci. USA*, **23**,1292–1299.
9 Dickerson,R.E., Drew,H.R., Conner,B.N., Wing,R.M., Fratin,A.V. and Kopka,M.L. (1982) *Science*, **216**, 475–485.
10 Chou,S.H., Flynn,D. and Reid,B.R. (1989) *Biochemistry*, **28**, 2422–2435.
11 Li,Y., Zon,G. and Wilson,W.D. (1991) *Biochemistry*, **30**, 7566–7572.
12 Zuo,E.T., Tanious,F.A., Wilson,W.D., Zon,G., Tan,G.-S. and Wartell,R.M. (1990) *Biochemistry*, **29**, 4446–4456.
13 Rinkel,L.J. and Altona,C. (1987) *J. Biomol. Struct. Dyn.*, **4**, 621–649.
14 Thibaudeau,C., Plavec, J., Garg,N., Papchikhin,A. and Chattopadhyaya,J. (1994) *J. Am. Chem. Soc.*, **116**, 4038–4043.
15 Tran-Dinh,S., Neumann,J.-M., Taboury,J., Huynh-Dinh,T., Renous,S., Genissel,B. and Igolen,J. (1983) *Eur. J. Biochem.*, **133**, 579–589.
16 Wüthrich,K. (1986) *NMR of Proteins and Nucleic Acids.* John Wiley & Sons, New York, NY.
17 Cantor,C.R. and Schimmel,P.R. (1980) *Biophysical Chemistry.* W.H.Freeman, San Franciso, CA.
18 Riazance,J.H., Baase,W.A., Johnson,W.C.,Jr, Hall,K., Cruz,P. and Tinoco,I.Jr (1985) *Nucleic Acids Res.*, **13**, 4983–4989.
19 Gray,D.M., Liu,J.-J., Ratliff,R.L. and Allen,F.S. (1981) *Biopolymers*, **20**, 1337–1382.
20 Lane,A.N., Jenkins,T.C., Brown,T. and Neidle,S. (1991) *Biochemistry*, **30**, 1372–1385.
21 Saenger,W. (1984) *Principles of Nucleic Acid Structure.* Springer, New York, NY.